

Imaging diagnosis of lumbar radiculopathy using
simultaneous MR neurography and apparent T2
mapping

(MR ニューログラフィーと T2 マッピングを
併用した腰椎神経根障害の診断)

千葉大学大学院医学薬学府

先進予防医学共同専攻

(主任：佐粧孝久教授)

佐藤 崇司

Abstract

We sought to assess the utility of simultaneous apparent T2 mapping and neurography with the nerve-sheath signal increased by inked rest-tissue rapid acquisition of relaxation-enhancement imaging (SHINKEI-Quant) for the quantitative evaluation of compressed nerves in patients with lumbar radiculopathy.

Thirty-two patients with lumbar radiculopathy and 5 healthy subjects underwent simultaneous apparent T2 mapping and neurography with SHINKEI-Quant. Regions of interest (ROIs) were placed in the lumbar dorsal root ganglia (DRG) and the spinal nerves distal to the lumbar nerves bilaterally at L4-S1. The T2 relaxation times were measured on the affected and unaffected sides. The T2 ratio was calculated as the affected side/ unaffected side. Pearson correlation coefficients were calculated to determine the correlation between the T2 relaxation times or T2 ratio and clinical symptoms. An ROC curve was used to examine the diagnostic accuracy and threshold of the T2 relaxation times and T2 ratio.

We observed no significant differences in the T2 relaxation times between the nerve roots on the left and right at each spinal level in healthy subjects. In patients, lumbar neurography revealed swelling of the involved nerve, and prolonged T2 relaxation times compared with that of the contralateral nerve. The T2 ratio correlated with leg pain. The ROC analysis revealed that the T2 relaxation time threshold was 127 ms and the T2 ratio threshold was 1.07.

To our knowledge, this is the first study to show the utility of SHINKEI-Quant for the quantitative evaluation of lumbar radiculopathy.

1. Introduction

Lumbar neuropathy causes low back and leg pain. However, findings on MRI have demonstrated abnormalities such as herniated nucleus pulposus and foraminal stenosis in 19% of asymptomatic subjects [1,2]. Furthermore, MRI can only identify morphological abnormalities, such as nerve disruption and narrowing, but cannot evaluate nerve damage quantitatively.

In degenerative lumbar spinal disorders, lumbar foraminal stenosis is a condition in which a nerve root or spinal nerve is entrapped in a narrowed lumbar foramen [3]. However, appropriately named the “hidden zone” by Macnab et al. [4], lumbar foraminal stenosis is often overlooked and plays a major role in lowering surgical success rates [5]. Diagnostic imaging of lumbar spinal canal stenosis involves a comprehensive review of X-rays, CT, and MRI [6–8], together with a functional diagnosis through selective nerve root imaging and infiltration [9]. Conventional MRI has been reported to produce false positives in 30 to 40% of lumbar foraminal stenosis cases, and therefore, it is a difficult condition to diagnose [10]. Thus, with conventional MRI, it is difficult to obtain a functional image diagnosis of the spinal nerves as well as the lumbar nerves branching from the spinal cord, and a new image diagnostic method is needed.

In recent years, with higher magnetic field strengths and improved pulse sequences, higher resolution neuroimaging has become possible. MR Neurography is a non-invasive and selective method to visualize peripheral nerves without contrast agents. Various methods such as 3D MR neurography, diffusion-weighted MR neurography, and diffusion tensor imaging (DTI) [11–15] have been reported. Diffusion tensor imaging is a quantitative MR imaging technique that can provide valuable information about tissue microstructural changes by measuring the anisotropy of water diffusion in vivo [16]. Although many studies have reported the use of DTI in lumbar nerve lesions [11–15], DTI of spinal nerve fibers is technically challenging due to their small size combined with the respiratory motion that may cause geometric distortions, and can induce variable tissue shifts [17,18].

MR neurography is a useful technique with which to visualize spinal nerves. Takahara et al. demonstrated MR neurography with diffusion-weighted imaging to visualize the brachial plexus [19,20]. The three-dimensional nerve-sheath signal can be increased with inked rest-tissue rapid acquisition of relaxation imaging (SHINKEI) [21], a new type of MR neurography that suppresses the signal from blood vessels, muscles, and fat tissue using improved motion-sensitized driven equilibrium (iMSDE) and spectral attenuated inversion recovery [21–25]. SHINKEI has been used to evaluate cervical nerve roots morphologically. However, a quantitative evaluation of involved nerve roots has not been reported.

Recently, Yoneyama et al. demonstrated an advanced sequence, SHINKEI-Quant [26], which can acquire MR neurography and simultaneously evaluate T2 relaxation times quantitatively. Hiwatashi et al. reported that patients with chronic inflammatory demyelinating polyneuropathy (CIDP) could

be distinguished from healthy subjects using SHINKEI-Quant [27,28]. Eguchi et al. have shown that the SHINKEI-Quant technique is useful for the quantitative evaluation of the injured nerve roots in cases of cervical radiculopathy [29].

However, to our knowledge, there has been no report using MR neurography with simultaneous apparent T2 mapping to evaluate lumbar radiculopathy. Therefore, the purpose of this study was to assess the utility of SHINKEI-Quant for the quantitative evaluation of compressed nerves in patients with lumbar radiculopathy due to disc hernia, foraminal stenosis, and spinal stenosis.

2. Methods

2.1. Participants

Informed consent was obtained from all participants prior to the study. The study protocol was approved by the ethical review committee (IRB number: H250-1). Thirty-two patients (16 male, 16 female, mean age 52.9 years, range: 24–82 years) with unilateral radicular symptoms including leg pain and 5 healthy subjects (all male, mean age: 37 years, range: 32–45 years) underwent simultaneous apparent T2 mapping and neurography with SHINKEI-Quant. Their diagnoses were based on neurologic symptoms, a selective nerve root infiltration, and a combination of diagnostic images including plain radiographs, CT, and MRI. This study included those patients in whom performing a selective nerve root infiltration diagnosed accurately the location of symptomatic nerve root. The patient group had 25 cases of lumbar disc herniation, 4 cases of lumbar spinal stenosis, and 3 cases of lumbar foraminal stenosis. The involved nerve root levels were 4 cases of L4 nerves, 18 cases of L5 nerves, and 10 cases of S1 nerves. Surgery was performed in 11 cases, which included 3 lumbar interbody fusions, 4 hernia extractions, and 4 intradiscal injections with condoliase (HERNICORE, Kaken Pharmaceutical Co. Ltd. Tokyo, Japan).

The clinical symptoms were assessed using the visual analogue scale (VAS) score for low back pain (LBP) and leg pain from 100 (extreme amount of pain) to 0 (no pain), leg numbness from 100 (extreme amount of numbness) to 0 (no numbness), and the Oswestry Disability Index (ODI) from 100 (the maximum disability possible) to 0 (no disability). The clinical evaluations were conducted prior to surgery and MR imaging.

2.2. SHINKEI-Quant imaging

We performed a detailed investigation of the affected nerves using SHINKEI-Quant imaging. The patients and healthy volunteers underwent MR imaging using a 3.0 T system (Ingenia CX; Philips, Best, the Netherlands) with a dStream Total Spine coil. Simultaneous T2 mapping and neurography

with SHINKEI-Quant was acquired in the coronal plane as a component of the lumbar nerve MR neurography protocol (Fig. 1A). The details of SHINKEI-Quant have been described elsewhere [15–19]. In brief, the protocol is turbo spin echo imaging with a diffusion-weighted prepulse called iMSDE to suppress the signal from blood vessels and muscles with a short tau inversion recovery fat-suppression prepulse. The prepulse is followed by a readout procedure with a tissue-specific, variable-refocusing, flip-angle rapid acquisition and a relaxation enhancement sequence to acquire contrast-efficient T2 weighting [15]. To synthesize the MR neurography and to estimate the apparent T2 relaxation time simultaneously, we applied two different iMSDE preparation times (sequences 1 and 2) interleaved (by TR) in a single acquisition. The SHINKEI parameters included TR/TE = 2200/100 ms, FOV = 300 × 300 mm, ETL = 90, acquisition matrix = 224 × 187, reconstructed voxel size = 0.60 × 0.60 × 2.00 mm³, b = 10 s/mm², iMSDE prep-time = 36 ms and 72 ms, and acquisition time = 6 min 36 s. The images were obtained in the coronal plane.

After MRI data were transferred to a PC, Extended MR Work Space software (Philips Medical Systems) was used for the T2 mapping.

The regions of interest (ROIs) were placed at two levels of the nerve root: proximal and distal to the lumbar foraminal zone. The T2 relaxation time was calculated by the software at two levels of the dorsal root ganglia (DRG) from L4–S1 in patients and healthy volunteers by two spine surgeons with 10 or more years of experience (YE and TS). The T2 ratio was calculated as the affected side/unaffected side. The size of ROIs ranged from 25 mm² to 50 mm² and was selected to be as close as possible to the respective nerve roots. The intra-observer (YE) and inter-observer reliabilities (YE vs TS) were also calculated.

2.3. Statistical analyses

All data are expressed as a mean ± standard deviation (MN ± SD). An unpaired t test was used to compare T2 values between the right and left sides of each DRG from L4 to S1. Pearson correlation coefficients were calculated to determine the correlation between the T2 relaxation times or T2 ratios and the clinical symptoms such as the VAS score and the ODI. An ROC curve was used to assess the diagnostic accuracy and to estimate the threshold of the T2 relaxation time and T2 ratio.

All analyses were performed using SAS Version 9.4 for Windows (SAS Institute Inc., Cary, NC, USA) and P < 0.05 was considered significant in all tests of statistical inference.

3. Results

Among healthy individuals, the mean T2 relaxation times at each spinal level were 122.0 ± 21.3, 110.7 ± 15.7, and 113.9 ± 28.3 for the L4, L5, and S1 nerve roots, respectively. There were no

significant differences in the T2 relaxation times at each spinal level ($p < 0.05$). We observed no significant differences in the T2 relaxation times for the nerve roots at each spinal level ($p < 0.05$). We also observed no significant differences in the T2 relaxation times between the nerve roots on the right and left sides (112.0 ± 19.4 , 119.0 ± 24.2 , $p = 0.48$) (Fig. 2). The intra-observer reliability for the T2 relaxation times was $r = 0.77$, and the interobserver reliability was $r = 0.78$.

The lumbar nerve T2 relaxation times (entrapped and intact sides) in the patients were DRG: 173.2 ± 39.9 , 124.5 ± 31.1 , $p = 9.2 * 10^{-7}$, and distal nerves: 118.2 ± 38.5 , 93.7 ± 26.3 , $p = 0.02$. Both the DRG and the distal nerve T2 relaxation times were significantly higher on the compression side than the intact side ($p < 0.05$) (Fig. 3).

The correlations with clinical symptoms are indicated in Figs. 4 and 5. The T2 relaxation times did not correlate with clinical symptoms (ODI: $r = 0.061$, $p = 0.741$; VAS for LBP: $r = -0.046$, $p = 0.804$; VAS for leg pain: $r = 0.159$, $p = 0.386$; VAS for leg numbness: $r = 0.099$, $p = 0.589$) (Fig. 4). However, the T2 ratio was correlated with the VAS for leg pain ($r = 0.366$, $p = 0.03$) but not with the other clinical symptoms (ODI: $r = 0.099$, $p = 0.591$; VAS for LBP: $r = 0.035$, $p = 0.848$; VAS for leg numbness: $r = 0.245$, $p = 0.176$) (Fig. 5).

The ROC analysis revealed that the T2 ratio was more accurate for the diagnosis of lumbar radiculopathy than the T2 relaxation time. The T2 relaxation time threshold was 127 ms (sensitivity: 90.6%, false positive: 43.8%, odds ratio: 12) and the T2 ratio threshold was 1.07 (sensitivity: 96.9%, false positive: 31.3%, odds ratio: 68) (Fig. 6).

A representative case of a 72-year-old woman is shown (Fig. 7A–D). Right leg pain appeared one month prior. At the initial visit, the clinical symptoms were: ODI = 31, VAS for LBP = 90, VAS for leg pain = 90, and VAS for leg numbness = 90. The MRI revealed L3/4 right intervertebral herniation (Fig. 7A, B). From the SHINKEI-Quant at the initial visit, the MR neurography indicated swelling of the right L4 nerve (Fig. 7C), and the T2 mapping indicated a DRG T2 relaxation time of 181 ms on the involved side and 97 ms on the intact side (Fig. 7D). A right L4 nerve root infiltration was performed and the VAS for leg pain was reduced from 90 to 50.

4. Discussion

We evaluated injured nerve roots quantitatively using SHINKEI-Quant in patients with lumbar radiculopathy due to disc hernia, foraminal stenosis, and spinal stenosis. Neurography revealed swelling of the involved nerves, and prolonged T2 relaxation times compared with that of the contralateral nerves. The T2 ratio, defined as the affected side/unaffected side, correlated with leg pain. The ROC analysis revealed that the T2 ratio was more accurate for the diagnosis of lumbar radiculopathy than the T2 relaxation time. The T2 relaxation time threshold was 127 ms and the T2 ratio threshold was 1.07.

Three-dimensional MR neurography has been used to evaluate entire nerves by providing better contrast between the nerves and the surrounding tissues. Recently, MR neurography has been increasingly used in patients with suspected lumbrosacral plexus involvement to help confirm the diagnosis or to provide anatomic information should surgical intervention be necessary [30]. However, this method can only demonstrate morphological abnormalities such as nerve disruption and narrowing, but cannot quantitatively evaluate nerve damage.

Diffusion weighted and diffusion tensor imaging are relatively new MR imaging techniques that measure the directional coherence of water diffusion in vivo. The fractional anisotropy (FA) values, calculated from DTI, were significantly lower and the apparent diffusion coefficient (ADC) values were significantly higher in entrapped roots compared to intact roots [15]. There were strong correlations between DTI parameters such as FA and indications of neurological severity including the Japanese Orthopedic Association (JOA) score, the Roland-Morris Disability Questionnaire (RDQ) [13], and the Oswestry Disability Index (ODI) [31]. DTI of the lumbar nerve can be used for the diagnosis, quantitative evaluation, and follow-up of lumbar nerve entrapment.

The SHINKEI-Quant technique can simultaneously provide both MR neurography and T2 mapping, which may help to quantitatively assess nerve pathology [26–29].

In comparison to DTI, the mean imaging time for DTI is 4 min and 54 s, and is 6 min and 36 s for SHINKEI-Quant. However, during DTI, the nerve is set as the ROI to create the tractogram and is depicted manually, whereas neurography is obtained automatically when using SHINKEI-Quant. Distortion is another issue that affects DTI; however the visualization of neurography is unaffected by distortion, giving the technique a major advantage. The use of DTI in lumbar nerve lesions can reveal with high accuracy, significant decreases in FA and significant increases in ADC values in compression lesions [15].

In this study, the T2 ratio, defined as the affected side/unaffected side, had higher diagnostic accuracy for radiculopathy than the T2 relaxation time alone. Although there is no previous report on the T2 relaxation ratio, we have previously tested the usefulness of lumbar spinal nerve diffusion tensor imaging (DTI) using DTI parameters for the affected side/unaffected side of the nerve at the same level [32]. The T2 ratio correlated with leg pain and may be more useful for distinguishing between individuals than T2 relaxation time alone.

A valuable study using SHINEKI-Quant found that the DRG and distal nerve root T2 relaxation times were longer in patients with chronic inflammatory demyelinating polyneuropathy (119 ms and 111 ms) than in healthy subjects (101 ms and 85 ms). Eguchi et al. evaluated injured nerve roots quantitatively using SHINKEI-Quant prior to microendoscopic surgery to treat a patient with cervical radiculopathy due to a cervical intervertebral disc herniation. SHINKEI-Quant imaging revealed swelling of the right C7 nerve, and a longer T2 relaxation time (127 ms) than that for the unaffected contralateral C7 nerve (74 ms) [29]. We performed microendoscopic surgery and the patient's

symptoms improved. SHINKEI-Quant technique is useful for quantitative evaluation of the injured nerve root in cases of radiculopathy. In the present study, the T2 relaxation times of the lumbar DRG in healthy volunteers were on average 115 ms, which is consistent with previous studies.

Karampinos et al. evaluated L4 nerves in humans and reported that the T2 relaxation times were significantly longer in the DRG (78.0 ms) than in more distal regions (59.5 ms) [33]. The times we observed were longer than those found in this previous study. SHINKEI-Quant calculates the T2 relaxation time using only two prep-times, which may have caused unstable assessments. The T2 relaxation time has been traditionally measured using multislice multiecho spin echo sequences, which might be a disadvantage for MR neurography. We compared the T2 relaxation times using 8 values (TE: 24, 48, 72, 96, 120, 144, 168, 192 ms) to those from 2 values (SHINKEI-Quant; TE: 36, 72 ms) in a rabbit spinal cord. The T2 relaxation times obtained from 8 values were 80 ms in grey matter and 100 ms in white matter, and the times obtained from SHINKEI-Quant (2 values) were longer by 10–20 ms than 8 values with stable assessments.

Electrophysiological tests to measure distal latency of the lumbar nerve have been reported as functional diagnostics. Distal latency delays occur in lateral lesions compared to medial lesions, allowing for differential diagnosis between medial and lateral lesions by this method. However, this is an invasive test and noninvasive diagnostic methods are virtually nonexistent [34,35].

We acknowledge that our study has several limitations. The first is the small number of subjects investigated. Second, we did not repeat the SHINKEI-Quant after surgery. We hope that by adding more cases, it will be possible to verify our findings. Third, due to the influence of motion artifacts in the abdomen, noise in the T2 mapping was observed, and it will be necessary to apply noise reduction strategies such as smoothing in future studies. There are few reports that include T2 relaxation times in patients with nerve injuries, and going forward, we will need to obtain more evidence with additional cases.

5. Conclusions

We evaluated injured nerve roots quantitatively using SHINKEI-Quant in patients with lumbar radiculopathy due to intervertebral disc herniation, foraminal stenosis, and spinal stenosis. Lumbar neurography revealed swelling of the involved nerves, and prolonged T2 relaxation times compared with that of the contralateral nerves. The T2 ratio, defined as the affected side/unaffected side, correlated with leg pain. When the T2 relaxation time and T2 ratio thresholds were established as 127 ms and 1.07, respectively, the accuracy was high for the diagnosis of lumbar radiculopathy. To our knowledge, this is the first study to show the utility of this technique to quantitatively evaluate lumbar radiculopathy.

6. Ethics and consent to participate

We declare that all protocols involving humans have been approved by the Shimoshizu National Hospital and Chiba University have been performed in accordance with the ethical standards laid down in the 1964 Declaration of Helsinki and its later amendments. We declare that all participants provided written informed consent before their inclusion in this study.

Conflicts of interest

The authors declare that they have no potentially competing interests. We did not receive grants or external funding in support of our research or preparation of this manuscript. We did not receive payments or other benefits or a commitment or agreement to provide such benefits from any commercial entities.

References

- [1] Boden SD, Davis DO, Dina TS, Patronas NJ, Wiesel SW. Abnormal magneticresonance scans of the lumbar spine in asymptomatic subjects. A prospective investigation. *J Bone Joint Surg Am* 1990;72(3):403–8.
- [2] Jensen MC, Brant-Zawadzki MN, Obuchowski N, Modic MT, Malkasian D, Ross JS. Magnetic resonance imaging of the lumbar spine in people without back pain. *N Engl J Med* 1994;331(2):69–73.
- [3] Jenis LG, An HS. Spine update. Lumbar foraminal stenosis. *Spine* 2000;25:389–94.
- [4] MacNab I. Negative disc exploration: an analysis of the causes of nerve root involvement in sixty-eight patients. *J Bone Joint Surg Am* 1971;53:891–903.
- [5] Burton R, Kirkaldy-Willis W, Yong-Hing K, Heithoff KB. Causes of failure of surgery on the lumbar spine. *Clin Orthop* 1981;157:191–7.
- [6] Hasegawa T, An H, Haughton V, Nowicki BH. Lumbar foraminal stenosis: critical heights of the intervertebral discs and foramina. *J Bone Joint Surg* 1995;77:32–8.
- [7] Kirkaldy-Willis W, Wedge J, Yong-Hing K, Tchang S, de Korompay V, Shannon R. Lumbar spinal nerve lateral entrapment. *Clin Orthop* 1982;169:171–8.
- [8] Vanderlinden RG. Subarticular entrapment of the dorsal root ganglion as a cause of sciatic pain. *Spine* 1984;9:19–22.
- [9] Herron L. Selective nerve root block in patient selection for lumbar surgery:surgical results. *J Spinal Disord* 1989;2:75–9.
- [10] Aota Y, Niwa T, Yoshikawa K, Fujiwara A, Asada T, Saito T. Magnetic resonance imaging and

magnetic resonance myelography in the presurgical diagnosis of lumbar foraminal stenosis. *Spine* 2007;32:896–903.

[11] Eguchi Y, Ohtori S, Orita S, Kamoda H, Arai G, Ishikawa T, et al. Quantitative evaluation and visualization of lumbar foraminal nerve root entrapment using diffusion tensor imaging: preliminary results. *Am J Neuroradiol* 2011;32:1824–9.

[12] Balbi V, Budzik JF, Duhamel A, Bera-Louville A, Le Thuc V, Cotten A. Tractography of lumbar nerve roots: initial results. *Eur Radiol* 2011;21 (6):1153–9.

[13] Eguchi Y, Oikawa Y, Suzuki M, Orita S, Yamauchi K, Suzuki M, et al. Diffusion tensor imaging of radiculopathy in patients with lumbar disc herniation: preliminary results. *Bone Joint J* 2016;98-B(3):387–94.

[14] Budzik JF, Vercllytte S, Lefebvre G, Monnet A, Forzy G, Cotten A. Assessment of reduced field of view in diffusion tensor imaging of the lumbar nerve roots at 3 T. *Eur Radiol* 2013;23:1361–6.

[15] Eguchi Y, Kanamoto H, Oikawa Y, Suzuki M, Yamanaka H, Tamai H, et al. Recent advances in magnetic resonance neuroimaging of lumbar nerve to clinical applications: a review of clinical studies utilizing diffusion Tensor Imaging and Diffusion-weighted MR neurography. *Spine Surg Relat Res* 2017;1 (2):61–71.

[16] Basser PJ, Jones DK. Diffusion tensor MRI: theory, experimental design and data analysis—a technical review. *NMR Biomed* 2002;15:456–67.

[17] Vargas MI, Viallon M, Nguyen D, Delavelle J, Becker M. Diffusion tensor imaging (DTI) and tractography of the brachial plexus: feasibility and initial experience in neoplastic conditions. *Neuroradiology* 2010;52:237–45.

[18] Chen YY, Lin XF, Zhang F, Zhang X, Hu HJ, Wang DY, et al. Diffusion tensor imaging of symptomatic nerve roots in patients with cervical disc herniation. *Acad Radiol* 2014;21:338–44.

[19] Takahara T, Hendrikse J, Yamashita T, Mali WP, Kwee TC, Imai Y, et al. Diffusion weighted MR neurography of the brachial plexus: feasibility study. *Radiology* 2008;249:653–60.

[20] Yamashita T, Kwee TC, Takahara T. Whole-body magnetic resonance neurography. *N Engl J Med* 2009;361:538–9.

[21] Yoneyama M, Takahara T, Kwee TC, Nakamura M, Tabuchi T. Rapid high resolution MR neurography with a diffusion-weighted pre-pulse. *Magn Reson Med Sci* 2013;12:111–9.

[22] Ogata H, Yamasaki R, Hiwatashi A, Oka N, Kawamura N, Matsuse D, et al. Characterization of IgG4 anti-neurofascin 155 antibody-positive polyneuropathy. *Ann Clin Transl Neurol* 2015;2:960–71.

[23] Hiwatashi A, Togao O, Yamashita K, Kikuchi K, Ogata H, Yamasaki R, et al. Evaluation of chronic inflammatory demyelinating polyneuropathy: 3D nerve-sheath signal increased with inked rest-tissue rapid acquisition of relaxation enhancement imaging (3D SHINKEI). *Eur Radiol* 2017;27:447–53.

[24] Hiwatashi A, Togao O, Yamashita K, Kikuchi K, Kamei R, Momosaka D, et al. Lumbar plexus

in patients with chronic inflammatory demyelinating polyneuropathy: evaluation with 3D nerve-sheath signal increased with inked rest-tissue rapid acquisition of relaxation enhancement imaging (3D SHINKEI). *Eur J Radiol* 2017;93:95–9.

[25] Kasper JM, Wadhwa V, Scott KM, Rozen S, Xi Y, Chhabra A. SHINKEI—a novel 3D isotropic MR neurography technique: technical advantages over 3DIRTSE based imaging. *Eur Radiol* 2015;25:1672–7.

[26] Yoneyama M, Togao O, Hiwatashi A, Ozawa Y, Obara M, Okuaki T, Causeren MV. SHINKEI quant: simultaneous acquisition of MR neurography and T2 mapping for quantitative evaluation of chronic inflammatory demyelinating polyneuropathy. *Proc Int Soc Magn Reson Med* 2016:1322.

[27] Hiwatashi A, Togao O, Yamashita K, Kikuchi K, Momosaka D, Nakatake H, et al. Simultaneous MR neurography and apparent T2 mapping in brachial plexus: evaluation of patients with chronic inflammatory demyelinating polyradiculoneuropathy. *Magn Reson Imaging* 2019;55:112–7.

[28] Hiwatashi A, Togao O, Yamashita K, Kikuchi K, Momosaka D, Nakatake H, et al. Lumbar plexus in patients with chronic inflammatory demyelinating polyradiculoneuropathy: evaluation with simultaneous T2 mapping and neurography method with SHINKEI. *Br J Radiol* 2018;91(1092):20180501.

[29] Eguchi Y, Enomoto K, Sato T, Watanabe A, Sakai T, Norimoto M, Yoneyama M, Aoki Y, Suzuki M, Yamanaka H, Tamai H, Kobayashi T, Orita S, Suzuki M, Inage K, Shiga Y, Hirokawa N, Inoue M, Koda M, Furuya T, Nakamura J, Hagiwara S, Akazawa T, Takahashi H, Takahashi K, Ohtori S. Simultaneous MR neurography and apparent T2 mapping of cervical nerve roots before microendoscopic surgery to treat patient with radiculopathy due to cervical disc herniation: preliminary results. *J Clin Neurosci* 2019. pii: S0967-5868(19) 31474-2.

[30] Soldatos T, Andreisek G, Thawait GK, Guggenberger R, Williams EH, Carrino JA, et al. High-resolution 3-T MR neurography of the lumbosacral plexus. *Radiographics* 2013;33(4):967–87.

[31] Wu W, Liang J, Ru N, Zhou C, Chen J, Wu Y, et al. Microstructural changes in compressed nerve roots are consistent with clinical symptoms and symptom duration in patients with lumbar disc herniation. *Spine* 2016;41(11):E661–6.

[32] Eguchi Y, Ohtori S, Suzuki M, Oikawa Y, Yamanaka H, Tamai H, et al. Discrimination between lumbar intraspinal stenosis and foraminal stenosis using diffusion tensor imaging parameters: preliminary results. *Asian Spine J* 2016;10:327–34.

[33] Karampinos DC, Melkus G, Shepherd TM, Banerjee S, Saritas EU, Shankaranarayanan A, et al. Diffusion tensor imaging and T2 relaxometry of bilateral lumbar nerve roots: feasibility of in-plane imaging. *NMR Biomed* 2013;26:630–7.

[34] Iwasaki H, Yoshida M, Yamada H, Hashizume H, Minamide A, Nakagawa Y, et al. A new electrophysiological method for the diagnosis of extraforaminal stenosis at L5–S1. *Asian Spine J* 2014;8(2):145–9.

[35] Ando M, Tamaki T, Kawakami M, Minamide A, Nakagawa Y, Maio K, et al. Electrophysiological diagnosis using sensory nerve action potential for the intraforaminal and extraforaminal L5 nerve root entrapment. *Eur Spine J* 2013;22:833–9.

[36] Brown R, Cheng Y-CN, Haacke E, Thompson M, Venkatesan R. Spin density, T 1, and T 2 quantification methods in MR Imaging. *Magnetic resonance imaging: physical principles and sequence design*. 2nd ed. John Wiley & Sons, Inc; 2014..

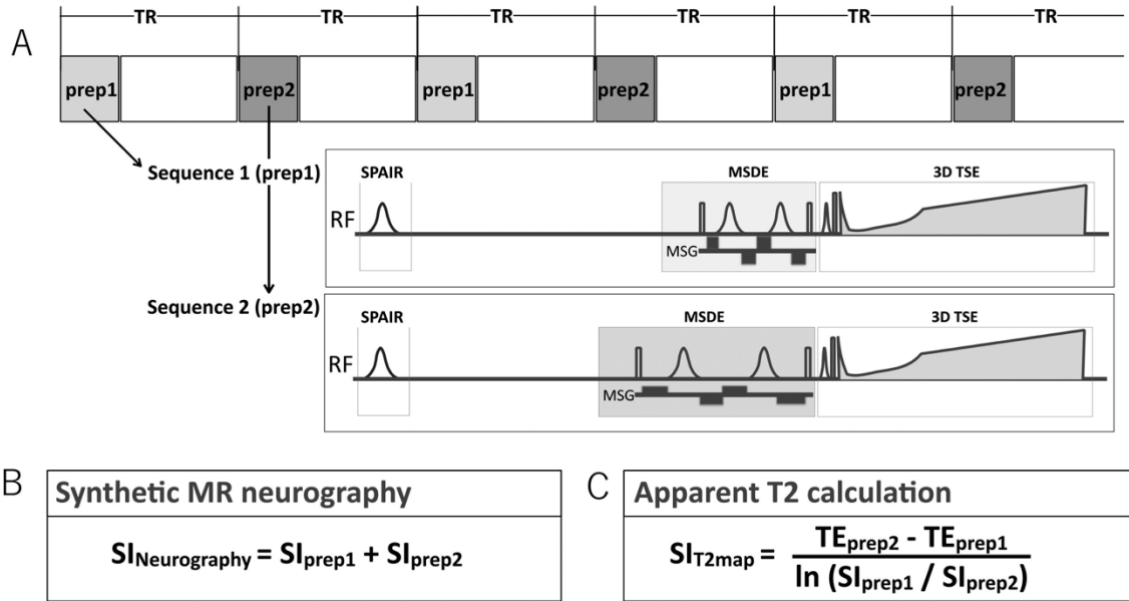


Fig. 1. A) Diagram of the sequences used in this study. SHINKEI consists of iMSDE, inversion-recovery-based fat suppression and 3D T2-weighted TSE sequences. Simultaneous MR neurography and apparent T2 mapping with SHINKEI interleaves (by TR) two different preparation times (sequences 1 and 2) into one acquisition for the synthesis of MR neurography and apparent T2 estimation. B) MR neurography was obtained with both iMSDE prep-times as follows: $SI_{\text{neurography}} = SI_{\text{preptime-1}} + SI_{\text{preptime-2}}$ where $SI_{\text{neurography}}$ indicates the signal intensity of the neurography, and $SI_{\text{preptime-1}}$, and $SI_{\text{preptime-2}}$ indicate the iMSDE durations of 36 and 72 ms, respectively. C) T2 mapping was calculated as follows: $SI_{T2\text{map}} = (TE_{\text{preptime-2}} - TE_{\text{preptime-1}}) / (SI_{\text{preptime-1}} / SI_{\text{preptime-2}})$ A T2 map was calculated by pixel-by-pixel fitting of the magnitude image intensities from both prep-times to a mono-exponential relaxation model [36].

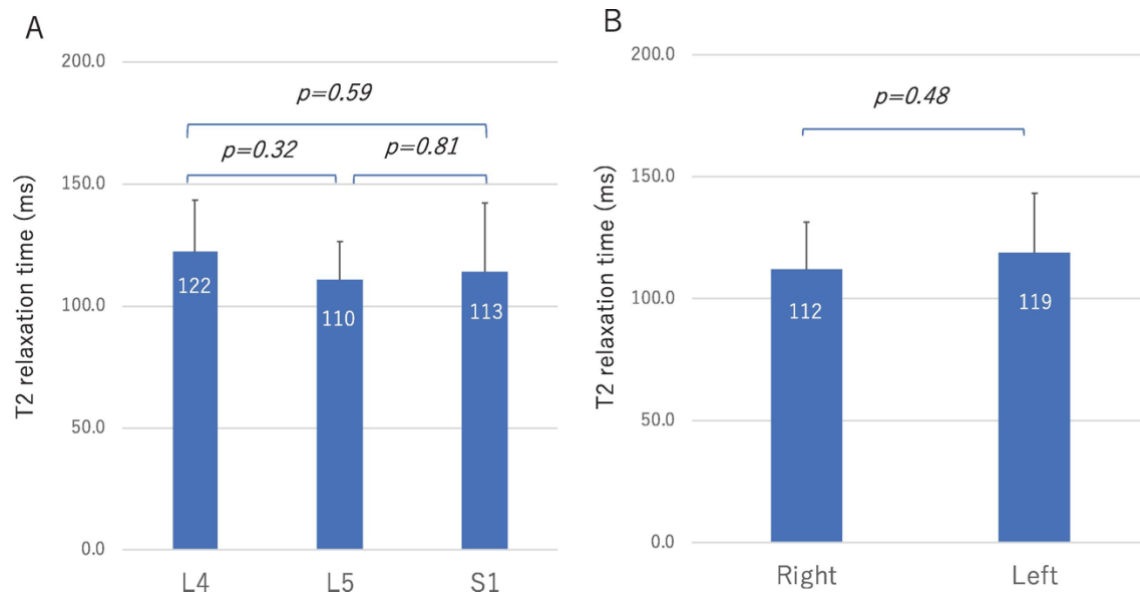


Fig. 2. Lumbar nerve DRG T2 relaxation times in healthy individuals. A) The mean T2 relaxation times at each spinal level were 122.0 ± 21.3 , 110.7 ± 15.7 , and 113.9 ± 28.3 for the L4, L5, and S1 nerve roots, respectively. There were no significant differences in the T2 relaxation times at each spinal level ($p < 0.05$). We observed no significant differences in the T2 relaxation times for the nerve roots at each spinal level ($p < 0.05$). B) The mean T2 relaxation times on the right and left sides were 112.0 ± 19.4 and 119.0 ± 24.2 . We also observed no significant differences in T2 relaxation times between the nerve roots on the right and left sides ($p = 0.48$).

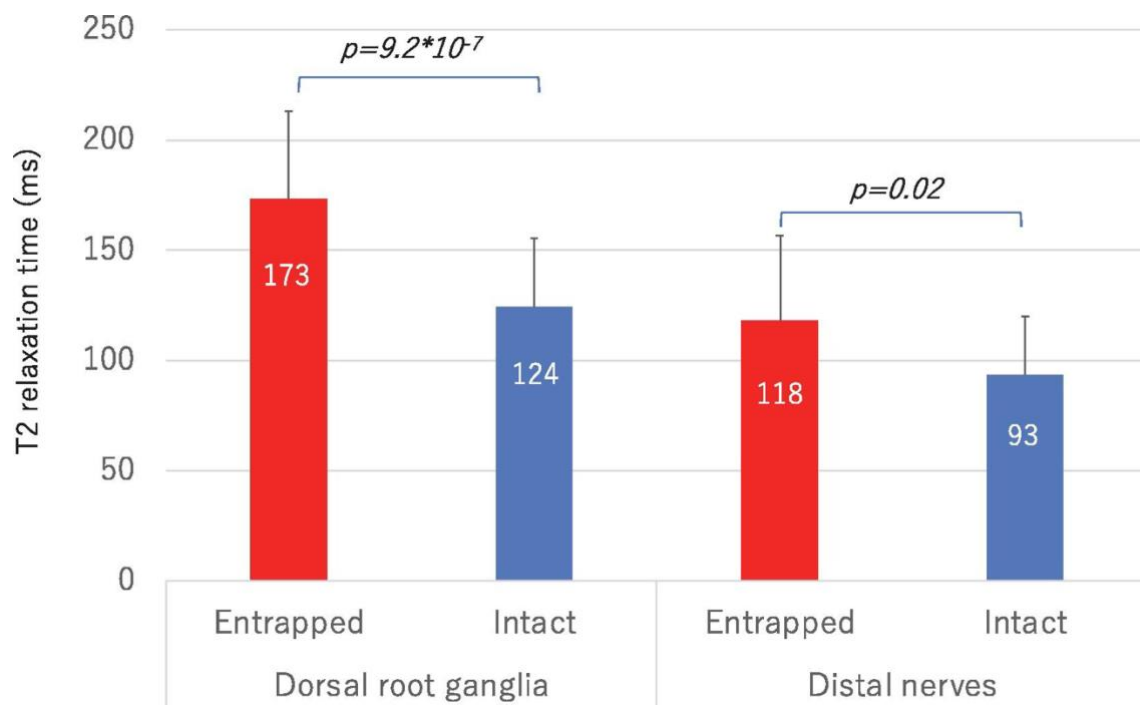


Fig. 3. The lumbar T2 relaxation times (entrapped and intact sides) in the dorsal root ganglia (DRG) and the distal nerves in patients are: DRG, 173.2 ± 39.9 , 124.5 ± 31.1 , $p = 9.2 * 10^{-7}$, and distal nerves, 118.2 ± 38.5 , 93.7 ± 26.3 , $p = 0.02$. Both the DRG and distal nerve T2 relaxation times were significantly higher on the compression side than the intact side ($p < 0.05$).

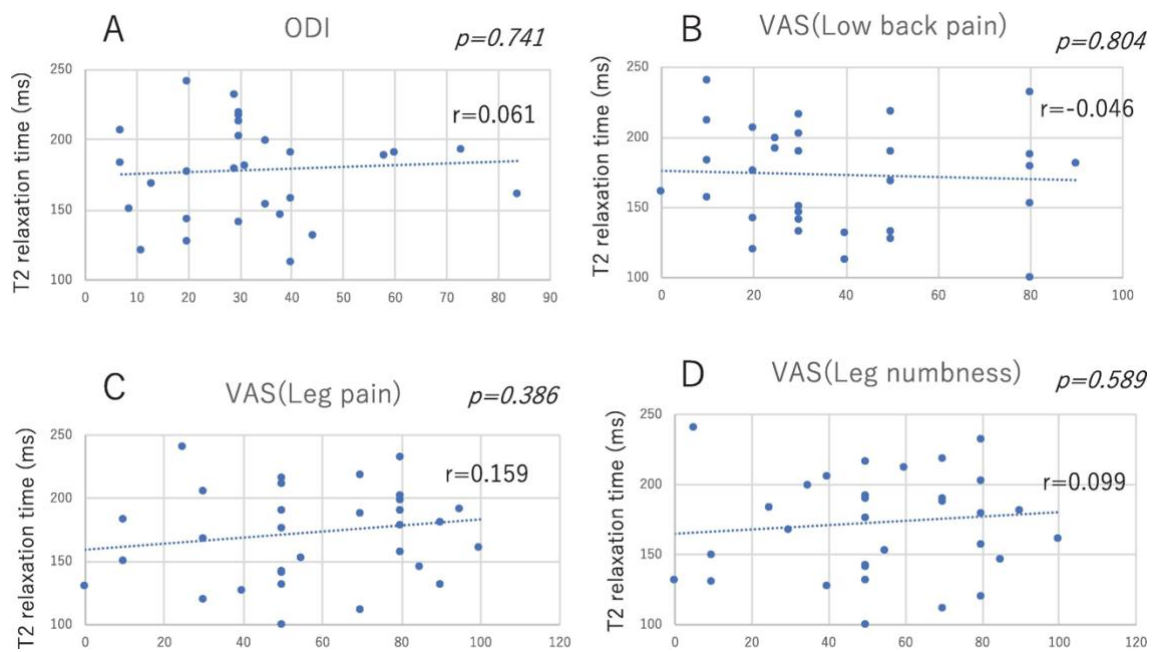


Fig. 4. The correlations between the T2 relaxation times and clinical symptoms. The T2 relaxation times did not correlate with clinical symptoms (ODI: $r = 0.061$, $p = 0.741$; VAS for LBP: $r = -0.046$, $p = 0.804$; VAS for leg pain: $r = 0.159$, $p = 0.386$; VAS for leg numbness: $r = 0.099$, $p = 0.589$).

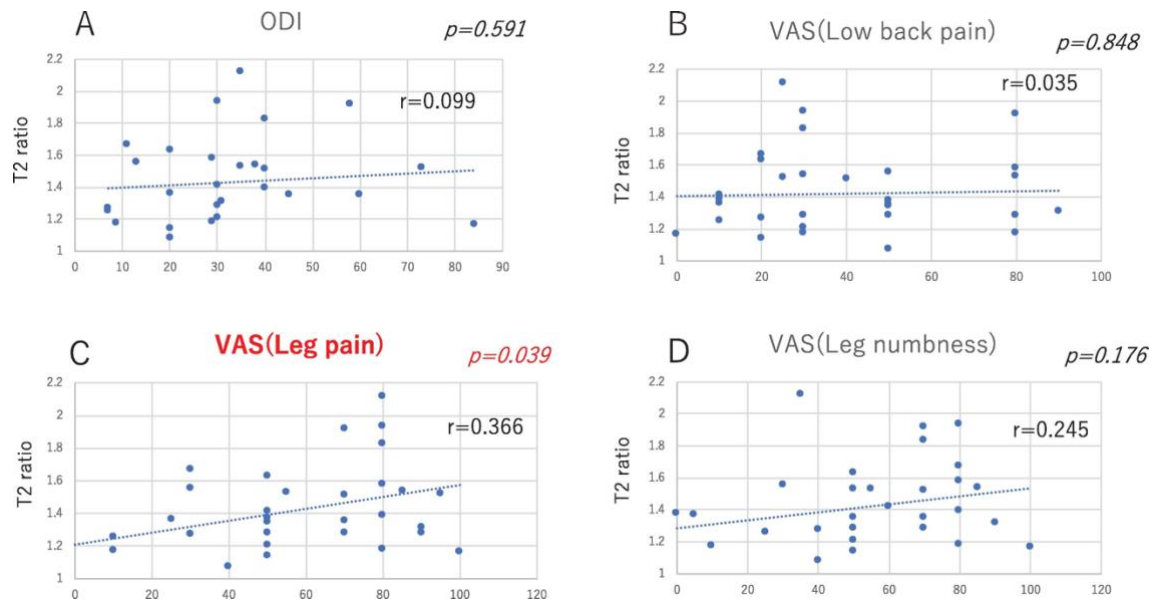


Fig. 5. The correlations between the T2 ratio and clinical symptoms. The T2 ratio was correlated with the VAS for leg pain ($r = 0.366$, $p = 0.03$) but not with the other clinical symptoms (ODI: $r = 0.099$, $p = 0.591$; VAS for LBP: $r = 0.035$, $p = 0.848$; VAS for leg numbness: $r = 0.245$, $p = 0.176$).

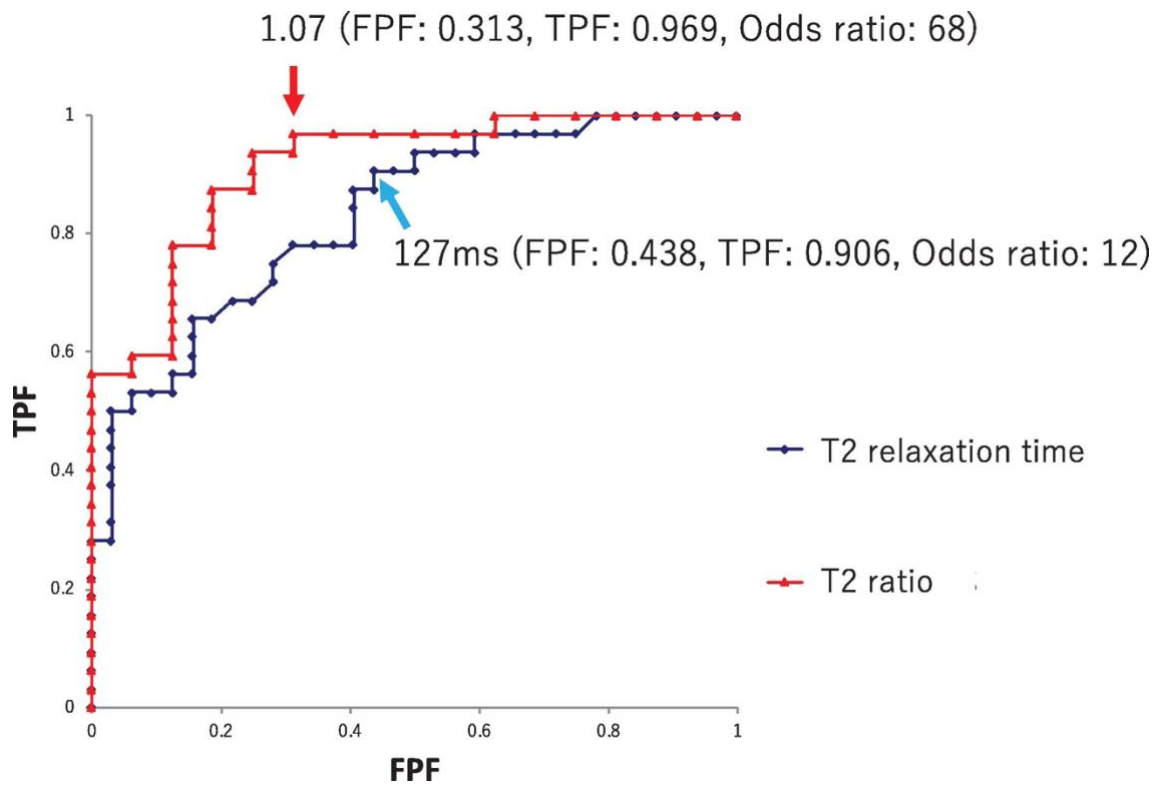


Fig. 6. The ROC analysis indicated that T2 ratio was more accurate for the diagnosis of lumbar radiculopathy than the T2 relaxation time. The T2 relaxation time threshold was 127 ms (sensitivity: 90.6%, false positive: 43.8%, odds ratio: 12) and the T2 ratio threshold was 1.07 (sensitivity: 96.9%, false positive: 31.3%, odds ratio: 68).

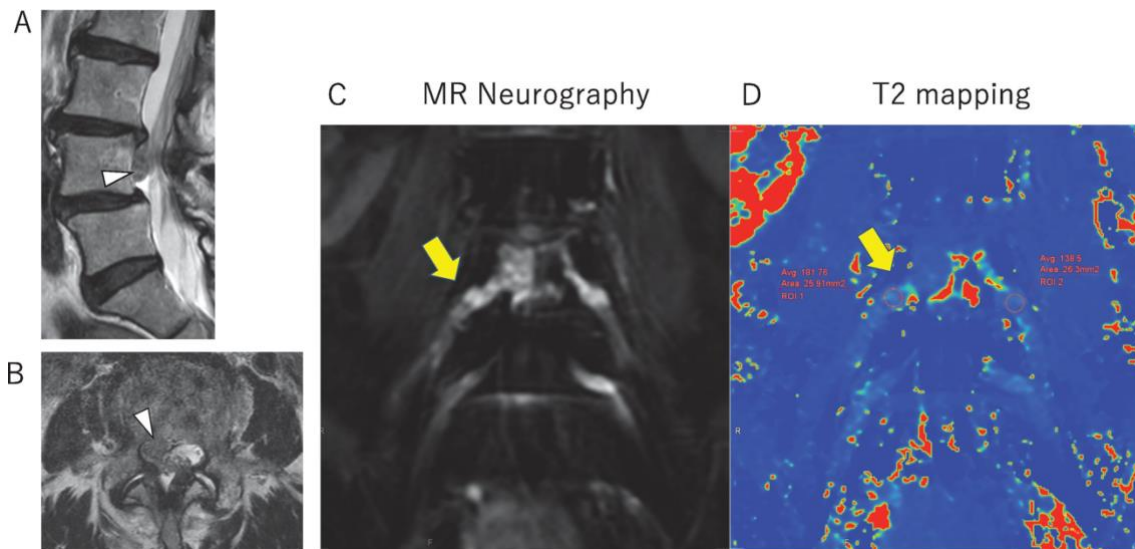


Fig. 7. A 72-year-old woman with lumbar intervertebral disc herniation. A, B) MRI (T2-weighted image) of the lumbar spine. A) Sagittal image. Herniation of the L3/4 intervertebral disc was observed (arrowhead). B) Axial image of L3/4. Right- side intervertebral disc herniation was observed (arrowhead). C) Lumbar MR neurography (coronal image) indicated swelling of the right L4 nerve (arrow), and D) Lumbar T2 mapping (coronal image) indicated that the DRG T2 relaxation time was 181 ms on the involved side and 97 ms on the intact side (increased on the involved side).

Journal of Clinical Neuroscience vol.78

2020年4月13日 公表済

DOI: 10.1016/j.jocn.2020.04.072.Epub 2020 Apr 24.